IEEE Access
Multidisciplinary | Rapid Review | Open Access Journal

Received December 13, 2020, accepted January 2, 2021, date of current version January 19, 2021.

Digital Object Identifier 10.1109/ACCESS.2021.3049485

A Cascading Failure Model Considering Operation Characteristics of the Communication Layer

GENG ZHANG[1,2], JIAWEN SHI[1], SHIYAN HUANG[1], JIYE WANG[2], AND HAO JIANG[1]
[1]Electronic Information School, Wuhan University, Wuhan 430072, China
[2]China Electric Power Research Institute, Beijing 100192, China

Corresponding author: Hao Jiang (jh@whu.edu.cn)

This work was supported in part by the National Natural Science Foundation of China Enterprise Innovation Development Key Project under Grant U19B2004, in part by the Equipment Project of the Equipment Development under Grant 41412010702, in part by the Major Research and Development Platform Project of New Research and Development Institutions in Zhongshan City under Grant 2017F1FC001, in part by the Special Funds for Innovation in Scientific Research Program of Zhongshan under Grant 181129112748101, in part by the Special Fund for Science and Technology of Guangdong Province under Grant 2019SDR002, and in part by the Key Project of Earth Observation and Navigation under Grant 2017YFB0504100.

ABSTRACT The coupling of communication networks plays an indispensable role in modern power systems; however, it also leads to many problems due to cascading failure. Although most current research focuses on the single-layer, non-interacting system and physical layer network, few studies have combined the complex network theory to ignore the influence of communication networks. To address this problem, this paper introduces a cascading failure model of a cyber physical power system (CPPS) that considers the operation characteristics of the communication layer, especially the influence of transmission delay and connectivity on stability control. First, the influence mode of the communication layer failure node acting on the physical layer is analyzed, and the interaction mechanism between the communication layer and physical layer is clarified. Furthermore, the propagation process of failure in the CPPS system is modeled, and the influence of information transmission delay on the stability control process is considered. In this manner, the development process of cascading failure in a CPPS system is described accurately. Finally, according to the loss rate of the physical layer load, the influence of the communication layer node is evaluated to verify the accuracy of the model. This paper also provides a practical model of a CPPS system, which is helpful for building a secure and reliable energy Internet.

INDEX TERMS Cascading failure, communication delay, complex network, cyber physical power system, stability control.

I. INTRODUCTION

As the energy Internet develops, the scale of power systems expands, and communication construction speed significantly improves. Modern power systems have gradually evolved into a communication coupling network composed of a physical power grid and communication network, or cyber physical power system (CPPS) [1]–[5]. CPPS is used to transfer useful data and control signals between the measurement point and the power system control center. As the independence between the communication layer and the physical layer increases, the CPPS enables the close correlation between computing, communication, and power resources.

The associate editor coordinating the review of this manuscript and approving it for publication was Chi-Tsun Cheng.

The communication layer provides sensing, communication, computing, and control support for the normal operation of the physical layer [6]. The physical layer supplies the energy needed for the operation of the communication layer equipment [7]; however, it also introduces new vulnerabilities: access to network attacks due to increased information sharing, risk of attacks on key equipment, and threats to reliable system operation. The coupling relation between layers makes system failure possible between the communication and physical layers, which could then cause a cascading failure [8]–[10]. Cascading failure is one of the most serious problems in power systems and may result in substantial economic losses and large-scale damage to power users [11]–[13].

To avoid these serious problems, recent research has studied the characteristics of cascading failure and has proposed

approaches from various angles to achieve improved precision in the CPPS cascading failure model. However, current research on this model is mostly focused on the physical layer [14]–[18]. For example, [19] introduces two types of transitions in cascading failure blackouts, including total generator capacity limits and power flow limits of network lines. Reference [20] has found that, in the physical failure transmission process, load distribution leads to the problem of power flow limitation. Other researchers such as [21] used the complex network theory and percolation theory to describe a dual-layer coupling model. [22] proposed a comprehensive model considering all the structures of the CPPS, including setting the random coupling strength between two layers. The majority of researchers believe that communication scheduling control behavior is completely reliable; however, communication network node failure may lead to the interruption of communication between nodes with some service transmission timeout and other known problems. Even though there are a few studies considering operational characteristics, [23] is the first attempt to model the interdependency between the networks with known topologies, while ignoring the influence of communication delay.

The critical aspect in the study of cascading failure is model authenticity relating to the effectiveness of the cascading failure process: 1) the physical layer determines the power grid structure and line power flow based on the law of Kirchhoff's voltage; 2) the communication layer determines the delay caused by process and transmission— real-time data determines the control command of the physical layer; 3) the coupling between the layers determines whether the physical layer has information dependence on the communication layer and the communication layer has power dependence on the physical layer, and whether the coupling strength is not 100%. [24]–[27] In this study, the cascading failure model based on existing research content was improved. The CPPS cascading failure model considers the running characteristics of the communication layer and studies the influence of decreasing network connectivity and increasing communication delay caused by communication node failure. This novel study focuses on the following:

1) We establish a two-layer model of a CPPS system considering communication transmission factors: system topology, energy flow transmission, information flow transmission, and inter-layer coupling relationships were considered comprehensively.

2) Based on the CPPS two-layer model, we analyzed the advantages and disadvantages of the existing classical percolation theory, and we proposed a cascading failure model of the CPPS that considered the operation characteristics of the communication layer, mainly the influence of information transmission delay on the effectiveness of stability control instructions during power system scheduling.

3) In our experiment, we calculated examples of a cascading failure model by examining the communication layer node used to measure the influence that a concrete synthesis method has on an IEEE 39 double network, an ER - ER double network, a BA -BA double network, and a WS - WS double network. We utilized a typical cascading failure model comparison to illustrate the accuracy of the model used for node influence assessment and the degree of differentiation.

The remainder of this paper is organized as follows: In Section II, we survey the existing cascading failure model described in the current literature; In section III, we abstract a CPPS model through relative knowledge and background and describe the running characteristics of each layer and the coupling relationships. Based on the CPPS model, we combine the communication characteristics into three phases of the failure process and analyze their influence on communication failure. In Section IV, we evaluate the performance of our model, and in Section V, we present the conclusion.

II. RELATED WORK

The establishment of a cascading failure model was originally conceived to reduce large-scale blackout and economic loss. Initially, many researchers established a model based on reductionism and differential algebraic equations; although the complex network theory was spread widely, a single network had been applied to the model simulation rather than an independent network. For example, in [28], a hidden failure model based on power law behavior was proposed, which prevented cascading failure overloads and subsequently led to increased system reliability and reduced blackout risk. [29] addressed two problems: attack-induced cascading breakdowns and the detection of range-based attacks on links, revealing vulnerabilities on real-world networks. None of these studies considered interacting networks or the running characteristics of each layer. Therefore, the limitations of these studies point out the need for a way to construct a more robust network.

To overcome the defects of reductionism, [21] first described the feasibility of a power grid dual-layer coupling network by applying complex network theory. Their research indicated that, compared to single networking, network coupling increased the vulnerability of the network. It set a precedent for studying the CPPS cascading failure model from the perspective of structural characteristics. Since then, studies based on this idea have focused on describing the structural characteristics of CPPS systems more accurately. [20] further considered that in the physical failure transmission process, load distribution leads to the problem of power flow limitation. This was contrary to the common infectious model where nodes only influence those nearby. The local node in a physical power grid failure may cause a remote power flow across limits, thus influencing a distant node. Without considering the possible influence of the communication layer and investigation on the coupling effect, it is difficult to accurately describe the failure process by modeling CPPS cascading failures based on only a physical layer [30]–[35]. Therefore, [23] considers the control role of the communication layer and the influence of the uninterruptible power system (UPS), which can schedule the power flow state of the physical layer and reduce the influence range of failure at the

physical layer. To some extent, UPS could block the influence of physical layer failure on the communication layer, but it is believed that the control function of the communication layer is completely reliable.

In fact, the communication layer is not a faultless or ideal model, and there are many normal factors limiting the running characteristics of the communication layer. [36] proposed that the failure of the communication layer may lead to a cascading failure in the power grid and introduces an improved cascading failure model that analyzes the dynamic process of communication failures in a wide-area protection system.

In contrast to other studies, we propose a cascading failure model considering the operation characteristics of the communication layer. It mainly considers the communication delay and stability control process sent to the physical layer, which more closely reflects actual circumstances.

III. THE PROPOSED MODE

This section comprehensively analyzes the CPPS system topology, power flow transmission characteristics, information flow transmission characteristics, and coupling relationships between layers. The CPPS system model is established and then proposed considering the working characteristics of the communication layer cascading failure model, and system communication and physical coordination failure processes are described.

A. THE CPPS MODEL

The CPPS system is a dual-layer coupling network that is deeply integrated between the physical power grid and the communication system [37]. Based on the topology, CPPS can be abstracted as a weighted undirected graph, and an adjacency matrix and a coupled edge matrix are used to represent the connection relationship between single-layer nodes and inter-layer nodes. The dynamic characteristics of the communication layer and physical layer are respectively modeled. The physical layer implements electrical energy transmission from power generation to electricity production. The communication layer monitors transmission between stations and control centers, notes differences in their transmission characteristics, and realizes system operations and evolution states through the dynamic superposition of discrete state information and continuous power processes. Figure 1 illustrates a section of network topology characteristics and the physical power flow transmission characteristics that establish the physical model G_p. Using the topological characteristics and communication business transmission characteristics, we establish a communication layer model, G_c. Starting from the inter-layer coupling relationship, E_D, the CPPS system model can be expressed as the physical, communication, and coupling matrices of collection $\xi\left(G_p, G_c, E_D\right)$.

1) PHYSICAL LAYER MODEL

The physical layer is the current-carrying part of the energy flow in the CPPS system that always calls the traditional grid. To simplify, only a high-voltage transmission network physical layer of 220 kV and above is considered, and the internal structure is ignored. Substations or power plants can be abstracted as nodes of the physical layer, and transmission lines can be abstracted as physical edges. Multiple lines in the unified direction can be merged to eliminate multiple edges and self-loops.

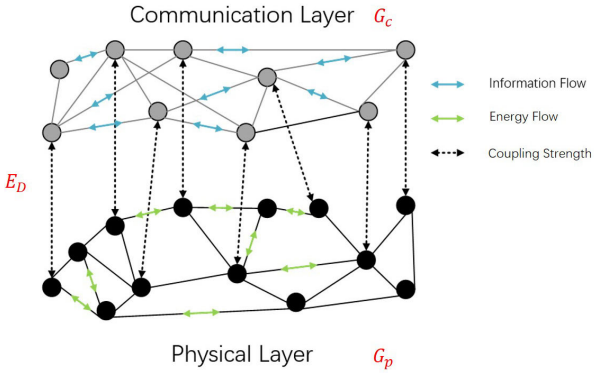

FIGURE 1. CPPS model.

The subscript p represents the CPPS power grid. The physical layer can be represented as the network $G_p(V_p, E_p)$ with N_p nodes and M_p edges and by the adjacency matrix $A_p = \left(r_{ij}\right)_{N_p \times N_p}$, where the adjacency matrix element is the reactance value, and the corresponding element is ∞ if no edges exist between nodes. The electric parameters of the nodes in the physical layer include generation output power, P_g, load power, P_l, phase angle, δ, and so on. The electric parameters of the connected edges include reactance r and line power flow power P, which meet Kirchhoff' s law of voltage and current. The power flow of the connected edges can be calculated according to the power of the nodes, the voltage of the balance nodes, and the phase angle as shown in Formula 3-1. The tolerance coefficient, γ, is defined to represent the relation $\gamma = P_{ij}^{Max} \Big/ P_{ij}$ between the limit of the connecting flow and the initial working current, which is generally set to 1.5.

$$\boldsymbol{P} = \boldsymbol{B}\boldsymbol{\delta} \tag{3-1}$$

2) COMMUNICATION LAYER MODEL

The subscript c represents the CPPS cyber network. The communication layer can be represented as the network $G_c(V_c, E_c)$ with N_c nodes and M_c edges, and by the adjacency matrix $A_c = \left(d_{ij}\right)_{N_p \times N_p}$, where the adjacency matrix element is the distance between nodes, and the corresponding element is ∞ if no edges exist between nodes.

This study mainly considers the influence of information transmission delay on the effectiveness of stability control instructions in power system scheduling. Figure 2 shows the reliability requirements of typical production control operations. Under a normal working state, the communication layer can meet the real-time requirements and business reliability needs of the transmission production control dispatch center.

Operation	Time delay	Real-time
Relay protection service	⩽10ms	Very high
Stability control service	⩽30ms	Very high
Dispatch automation service	⩽100ms	Very high
Wide area measurement service	⩽30ms	High
Dispatching telephone	⩽150ms	High
Safety monitoring service	Second level	Low
Power metering telemetry	Second level	Low
Fault recording	Minute level	Low

FIGURE 2. Reliability requirements of production control business.

Through access to system information at each station terminal, if there is a limitation or imbalance in power flow at the physical layer, the stability control is implemented, and feedback control information is communicated to the system to achieve ''closed-loop control.'' However, when the communication layer is damaged, the connectivity of the communication layer decreases, and the delay of circuitous routes increases. The dispatching center cannot perceive the system condition correctly; therefore, it makes improper decisions. As a result, monitoring and control abilities are weakened and failure spreads further. Therefore, the effectiveness and real-time performance of the control instructions in the communication layer as well as the production control business exchange processes are the basic operational requirements.

The key factor affecting the validity of the communication layer data is whether the dispatching center can accurately perceive the actual state of the physical power grid. To represent the influence of communication layer damage on the decision-making effectivity of the system, the physical layer state information obtained by the communication layer scheduling center through situational awareness is defined as the physical layer mirror model G_p^j.

$$\boldsymbol{G_p^j = G_p - \Delta G_p} \tag{3-2}$$

where G_p is the actual state of the physical layer, and ΔG_p is the acquisition error. The communication layer dispatching center updates the database in real time according to the information collected by the terminal of the plant and forms the physical layer mirror model. The electrical parameters of the mirror model indicate that there is a line power flow overshoot or power imbalance in the physical layer. The dispatching center performs optimization calculations according to the electrical parameters of the mirror model to generate stability control instructions. The objective function and constraint conditions are shown in Equations (3-3) through (3-7). $f_{LL}(G)$ expresses current control strategy system load reductions, F_k represents the trend on line k, LS_u expresses cutting load on node u, P_g^{Min} and P_g^{Max} represent the minimum and maximum power, respectively, P_{uv} denotes the line tide between nodes u and v, P_{uv}^{Max} expresses the maximum capacity that the corresponding line allows in a short time, and L_u is the load of node u.

$$\min f_{LL}(G) \tag{3-3}$$

$$\sum\nolimits_{k\in in(u)} F_k - \sum\nolimits_{k\in out(u)} F_k + \sum\nolimits_{g\in g(u)} P_g = L_u - LS_u \tag{3-4}$$

$$P_{uv} = B_{uv}(\delta_u - \delta_v) \tag{3-5}$$

$$P_g^{Min} \le P_g \le P_g^{Max} \tag{3-6}$$

$$P_{uv} \le P_{uv}^{Max} \tag{3-7}$$

The transmission delay of the communication route is the key factor affecting the real-time performance of the communication layer. Considering the sufficient bandwidth of the backbone optical transmission network and the strong data-forwarding ability of optical transmission equipment, the influence of communication congestion is not considered in this study. There are two main aspects of the service end-to-end transmission delay: optical transmission equipment processing delay and optical fiber link transmission delay. The delay formula of the communication layer service from source node u to target node v is as follows:

$$T(u,v) = 2T_1 + T_2 \times N(u,v) + \frac{Ln_1}{c} \tag{3-8}$$

T_1 is the transmission delay of upper and lower equipment in the service; T_2 is the transmission delay of intermediate equipment, which is approximately $10\mu s$. $N(u, v)$ is the total equipment between node u and target node v; c is the speed of light in vacuum ($3 \times 10\text{^}5\ km/s$); L is the transmission distance; and n_1 is the refractive index of the optical fiber, with a typical value of 1.48.

3) COUPLING RELATIONSHIP

The coupling relationship between the communication layer nodes and physical layer nodes in the CPPS system is the basis of the interaction between the communication space and physical grid. The coupling relationship changes dynamically with the operation state of the CPPS system [9], [38]–[41]. On one hand, the function and shape of CPPS system nodes are different; thus, there are many connection types, such as one-way tight coupling, one-way loose coupling, and two-way loose coupling. On the other hand, in different states of the CPPS system, the coupling between nodes can be ''connected and active'' (working properly), ''disconnected and active'' (single-layer failure), and ''disconnected'' (total failure). This coupling relationship can be abstracted into two processes: information transmission and energy supply. Specifically, the information transmission process is a two-way action relation that represents the information acquisition process of the physical power grid and the stability control process of the communication layer to the physical layer, while the energy supply process is a one-way action relation in which the physical power grid provides the necessary energy source for the normal operation of various intelligent terminals in the communication space. The communication

and the physical layer nodes often have a master-slave relationship, and based on this "one-to-one" corresponding relation, the simulation model is set up.

This novel study uses the concept of a coupling edge to describe the information and energy exchanges between the communication layer and physical layer and defines the directivity and coupling strength of the coupling edge to describe various coupling relations existing in the power system. According to the direction of the coupling side, the coupled side matrix representing the communication layer and the physical layer of the power system includes the information dependence of the physical grid on the information network and the energy dependence of the information network on the physical grid. The coupling strength of the inter-layer nodes is reflected by the coupling edge matrix E_D. The matrix element $\rho_{u-v}\rho_{u-v}$ is $0 \leq \rho_{u-v} \leq 1$. E_D represents $E_D = \{E_{c-p}, E_{p-c}\}$, where $E_{c-p}E_{c-p}$ represents the coupled side matrix of the information network depending on the physical network, and $E_{p-c}E_{p-c}$ represents the coupled side matrix of the physical network depending on the information network. The matrix elements represent the coupling strength of the normal operation of the communication layer and power nodes.

B. SYSTEM CASCADING FAILURE MODEL

To facilitate the determination of the working state of nodes in each layer during cascading failure development, the following assumptions are made in this section for the simulation scenario and node state: 1) In this study, a scheduling center is set up in the communication layer; it is assumed that it has high reliability, is not affected by system failure, and can maintain normal operation. 2) The DC power flow equation is used to calculate the steady-state electrical parameters of the physical layer nodes in the development of cascading failure without considering the transient process after failure occurrence. 3) If the communication layer nodes continue connecting with the dispatching center and the coupling physical layer nodes have not failed, the communication layer nodes are working normally; if the communication layer nodes continue connecting with the dispatching center but the coupling physical layer nodes have failed, the communication layer nodes are in a high-risk working state that can cause probabilistic failure in each iteration. The probability is equal to the coupling strength ρ. 4) If the physical layer nodes belong to the maximum working connected subset or "power island" and the coupled communication layer nodes have not failed, the physical layer nodes are working normally; conversely, if the coupling communication layer nodes have failed, the physical layer nodes are in a high-risk working state that can cause probabilistic failure in each iteration. The probability is equal to the coupling strength ρ.

Figure 3 shows the complete implementation process.

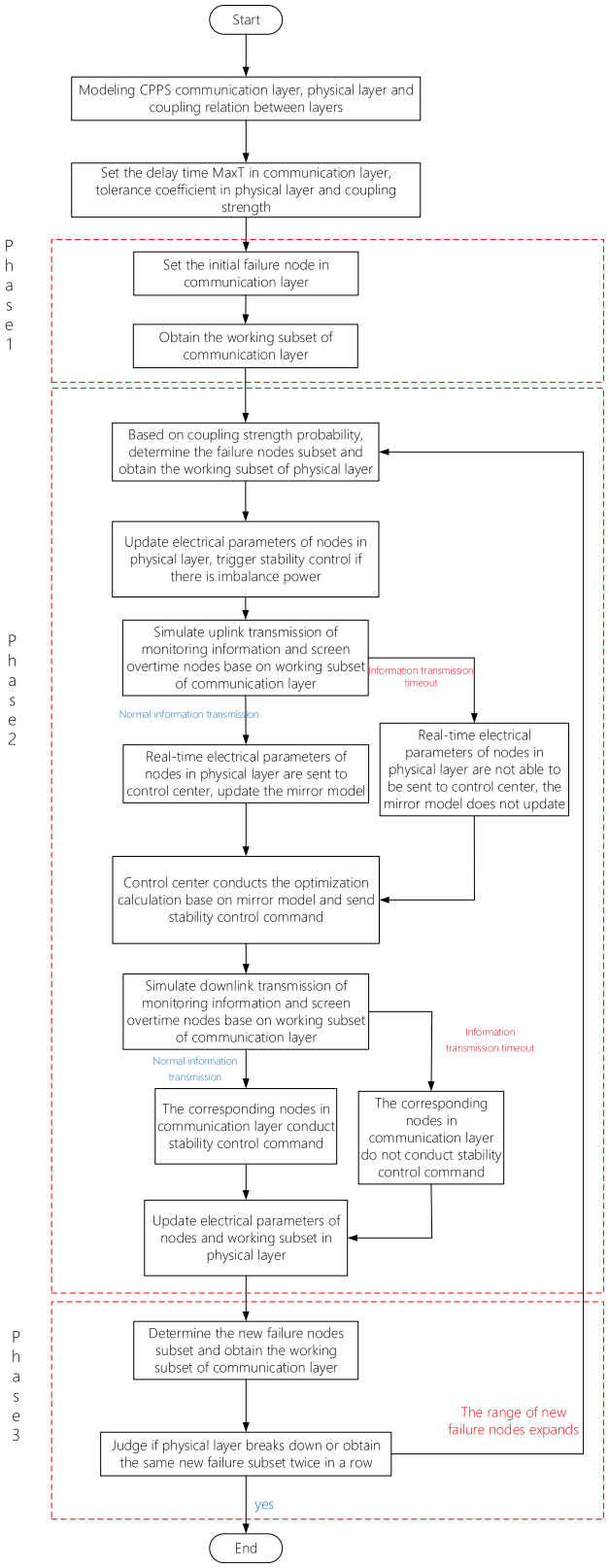

FIGURE 3. Cascading failure model.

1) INITIAL FAILURE

Some nodes in the communication layer fail because of equipment aging, hardware defects, attacks, and so on. The failure of nodes leads to a decrease in communication layer connectivity. The communication layer nodes $N_{c0}^{\sim}$ after the initial

failure nodes are removed can be expressed as

$$N_{c0}^{\sim} = B_{\mu_0}(\mu_0, N_c) \tag{3-9}$$

N_c represents the original system communication layer node set, and μ_0 represents the initial failure node set. $B_{\mu_0}(\mu_0, N_c)$ calculates the complement set of μ_0 in the universal set N_c.

The normal operation of the communication layer nodes requires communication with the scheduling center to determine whether complement nodes relate to the scheduling center and to obtain the working subset of the communication layer after the initial failure nodes are removed. The operation is represented as

$$(G_{c0}, N_{c0}) = F(G_c, N_{c0}^{\sim}) \tag{3-10}$$

In the original communication layer network G_c, the Floyd–Warshall algorithm is used to calculate the shortest distance between nodes in the node set $N_{c0}^{\sim}$ and the scheduling center [42]. The shortest distance is infinite, indicating that there is no effective connection between the node and the scheduling center. This node and its associated edges are removed from the network, and the communication layer working subsets, N_{c0}, and the communication layer network, G_{c0}, are finally obtained after the initial failures.

2) PHYSICAL LAYER FAILURE ANALYSIS

The initial failure of the communication layer diffuses to the physical layer through the interlayer coupling relationship—the connectivity and electrical properties of the physical layer change. If there is power flow across the limit or power imbalance in the lines, the dispatching center conducts stability control according to the power parameters that can be monitored. Presently, if the decline in connectivity of the communication layer increases or decreases the transmission delay, and some information cannot be effectively transmitted, the optimal stability control effect cannot be obtained. The operations involved include identifying the physical layer working subsets and simulating stability control processes.

• **Identifying physical layer working subsets:** The physical layer nodes corresponding to the newly added failure nodes in the communication layer are removed from the physical layer working subset based on the coupling strength probability. The set of remaining nodes is represented as

$$N_{p11}^{\sim} = B_{\rho\upsilon_1}(\rho\upsilon_1, N_p) \tag{3-11}$$

υ_1 is the set of nodes on the physical layer coupled to the communication layer's new failure nodes. N_p is the working subset of the physical layer, and $B_{\rho\upsilon_1}(\rho\upsilon_1, N_p)$ is the complement calculation. The normal operation of physical layer nodes needs to be in the operational "power island." The connected components of the physical layer network are obtained by the Tarjan algorithm. According to the DC power flow equation, the generation power in the connected component can be judged to meet all or part of the load demand. The maximum connected component that meets the demand is defined as the "main network," and the other connected components that meet the demand are "power islands." Nodes belonging to the "main network" and "power islands" constitute the working subset of the physical layer, thus removing nodes that are not part of the working subset and node-related edges from the physical layer network. We define $K(G_p, N_{p11}^{\sim})$ in the operation above to obtain the working subset node N_{p11} and the physical layer network G_{p11}.

$$(G_{p11}, N_{p11}) = K(G_p, N_{p11}^{\sim}) \tag{3-12}$$

• **Simulating stability control processes:** The communication layer working nodes collect the electrical parameters of the physical layer nodes and send them to the dispatching center, and the transmission delay of the acquired information is calculated. A transmission delay that is greater than the delay threshold $MaxT$ is considered as a transmission failure. This requirement is given in Figure 2. The corresponding data in the physical layer image model is not updated. N_{p12}^{j} represents the set of nodes at the physical layer that can be detected by the scheduling center and meets the following requirements:

$$N_{p12}^{j} \leq N_{p11} \tag{3-13}$$

According to the information received, the dispatching center takes the minimum load loss as the objective function to carry out an optimization calculation and defines $SC(P_{12}^{j}, N_{p12}^{j})$ to represent the stability control operation of updating electrical parameters.

$$P_{12}^{j\sim} = SC(P_{12}^{j}, N_{P12}^{j}) \tag{3-14}$$

P_{12}^{j} represents the electrical parameters in the physical layer mirror model of the dispatching center, and $P_{12}^{j\sim}$ represents the electrical parameters after stability control.

The dispatching center updates the electrical parameters to the working nodes of the communication layer along with the control instruction. A control information transmission failure occurs when the transmission delay is greater than the threshold $MaxT$, and the node receiving the control information adjusts the electrical properties according to $P_{12}^{j\sim}$. The power flow calculation of the physical layer power grid was performed again, severely overloaded lines were cut out, and the working subset of the physical layer was updated to obtain the working subset N_{p1} and the physical layer network G_{p1}.

$$(G_{p1}, N_{p1}) = K(G_{p11}, N_{p11}) \tag{3-15}$$

3) COMMUNICATION LAYER FAILURE ANALYSIS

New physical layer failure nodes cause the coupling communication layer node to lose energy depending on a probability. The probability of failure is the coupling strength, removed from the working connected subset of the communication layer. In Phase 1, the Floyd-Warshall algorithm is used to confirm the communication layer working nodes set N_{c1} and

the communication layer network G_{c1}.

$$N_{c1}^{\sim} = B_{\rho\mu_1}(\rho\mu_1, N_{c0}) \tag{3-16}$$

$$(G_{c1}, N_{c1}) = F(G_{c0}, N_{c1}^{\sim}) \tag{3-17}$$

The CPPS cascading failure development process can be summarized as a continuous iterative process between Phase 2 and Phase 3 triggered by the initial node failure of Phase 1. Formula 3-15 outputs the physical layer working subsets N_{p1} and physical layer network G_{p1} at the end of each iteration, and Formula 3-17 outputs the communication layer working subsets N_{c1} and communication layer network G_{c1} at the end of each iteration; these are used as inputs for iterations 3-11, 3-12, 3-16, and 3-17. After the end of each iteration, if there are no new failure nodes in the results of the previous iteration or system physical layer collapse. Then, the cascading failure iteration process ends, and the influence of nodes is calculated.

IV. EXPERIMENT ANALYSIS

To express the accuracy and discrimination of our model, this section implements experiments in the IEEE 39 dual-layer network, ER-ER dual-layer network, BA-BA dual-layer network, and WS-WS dual-layer network, we compare proposed model to three typical cascading failure models: Brummitt model [20], the Buldyrev model [21], and Korkali model [22].

A. EXPERIMENT NETWORK AND ENVIRONMENT

In this study, experiments were conducted on four types of CPPS datasets with different structural characteristics: the IEEE 39 nodes system, ER random network model, BA scale-free network model, and WS small world network model. Through the MATLAB MATPOWER function, we called the IEEE 39 system whose nodes and lines information are shown in Figure 4(a). The IEEE 39 node system is composed of 10 generator nodes, 21 load nodes, 12 transformer nodes, and 46 transmission lines. The topological structure of the system is shown in Figures 4(b). This study constructs the communication layer topology based on the IEEE 39 node system topology. The nodes on the communication layer correspond to the nodes on the physical layer, and then ten percent of the links in the communication layer are reconnected randomly without links, which leads to self-looping or repetition. Considering the communication delay from each node to the dispatching center, this study chose the node with the shortest average path to act as the dispatching center.

To fully consider the influence of topology characteristics on the accuracy of the cascading failure model, this study synthesizes the ER-ER dual-layer network, the BA-BA dual-layer network, and the WS-WS dual-layer network based on the ER random-network model, BA scale-free network model, and the WS small-world network model, respectively. The concrete synthesis method is as follows: first, a physical layer network with the same scale as the IEEE 39 system is generated, and the electrical parameters of IEEE 39 system

Component	Number
Buses	39
Generators	10
Committed Gens	10
Load nodes	21
Fixed	21
Dispatchable	0
Shunts	0
Transmission lines	46
Transformer nodes	12
Inter-ties	6
Areas	3

(a)

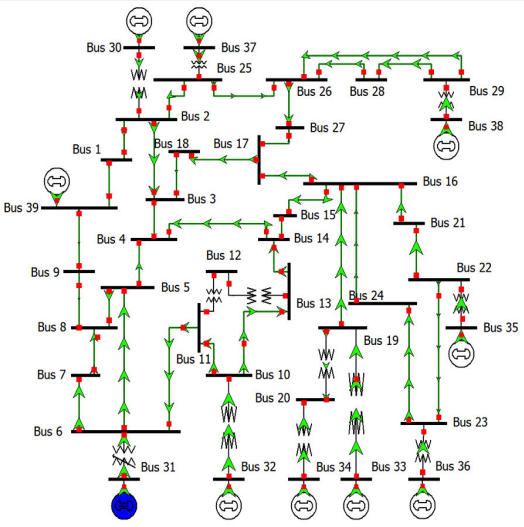

(b)

FIGURE 4. Information of IEEE39.

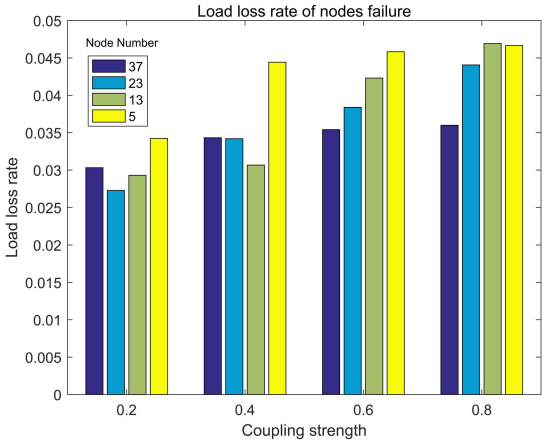

FIGURE 5. Influence assessment results of some nodes in IEEE 39 dual-layer system.

nodes are randomly assigned to new network nodes. Second, the power flow at the edge of the physical layer network is calculated as the initial power flow according to the generation and load of the nodes. Finally, the "one-to-one" corresponding communication layer network is generated, the coupling relationship is established, and the link of a few communication layers is reconnected. The link connection weight of the communication layer is the random assignment

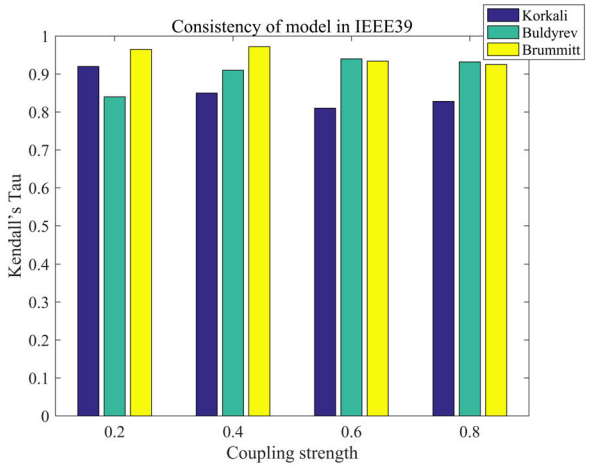

(a) Consistency τ value for the IEEE 39 dual-layer system model

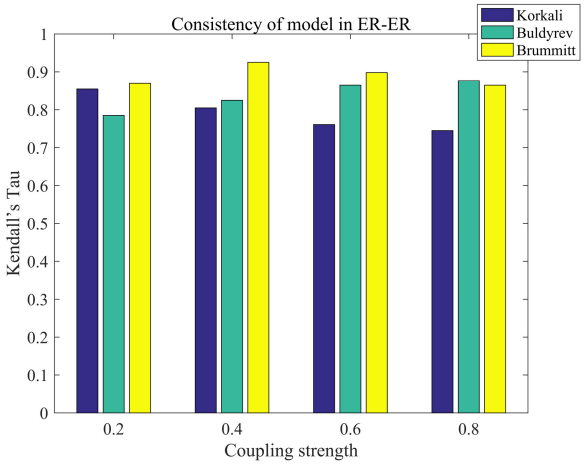

(b) Consistency τ value for ER-ER dual-layer system model

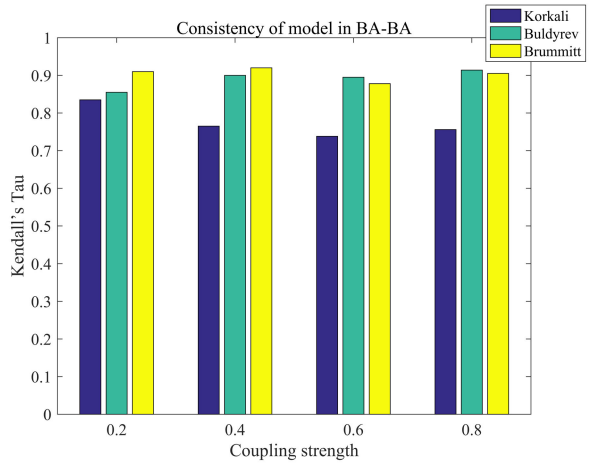

(c) Consistency τ value for the BA-BA dual-layer system model

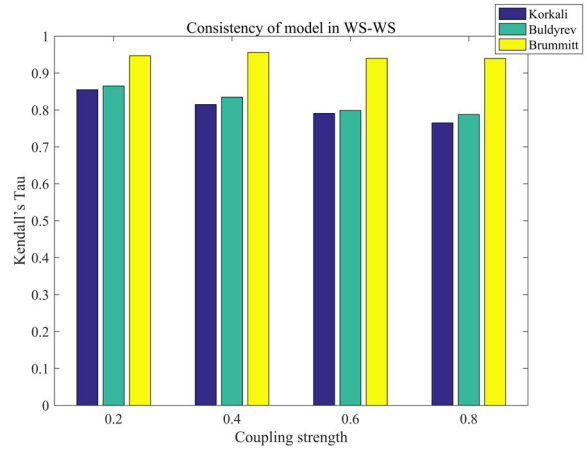

(d) Consistency τ value for the WS-WS dual-layer system model

FIGURE 6. τ **values of the model in this paper and different models in different systems.**

of node communication distance under the condition that the initial delay is less than the delay threshold MaxT (u, v).

The model implementation platform consisted of Python and MATLAB. Python partially realizes the two functions of CPPS system generation and coupling iteration, while MATLAB partially realizes four functions: parameter input, failure setting, physical layer power flow calculation, and influence calculation. Python and MATLAB call each other through command line instructions, share comma-separated values (CSV) file data, and realize power flow calculation with the help of MATPOWER, an open-source power system simulation package provided by MATLAB [43].

B. IMPACT MEASUREMENT INDEX

When cascading failure is terminated, the load loss of the physical layer represents the influence of node failure on the system transmission function. Therefore, this study measures the influence of node failure from the perspective of system function loss and defines the load loss rate R_{LL}, whose value is the proportion of cascading failure loss load in the initial load of the physical layer. Equation 4-1 gives the specific formula.

$$\boldsymbol{R_{LL}} = \mathbf{1} - \sum_{i \in N_p^{final}} \boldsymbol{P_{li}} \Big/ \sum_{i \in N_p^{initial}} \boldsymbol{P_{li}} \qquad (4\text{-}1)$$

In the formula, P_{li} represents the load of node i, $N_p^{initial}$ is the working subset of the initial physical layer nodes, and N_p^{final} is the working subset of the physical layer nodes when the cascading failure terminates.

C. SIMULATION RESULTS ANALYSIS

To measure node influence using the cascading failure model, after setting the initial failure of the node, we obtained the loss rate of the physical layer load as node influence. Owing to the existence of coupling strength, there is randomness in the results; thus, it is necessary to take the average value for multiple simulations. The following are the results of 100 simulations. In the IEEE 39 dual-layer system, the influence assessment results of some nodes obtained using the cascading failure model are shown in Figure 5.

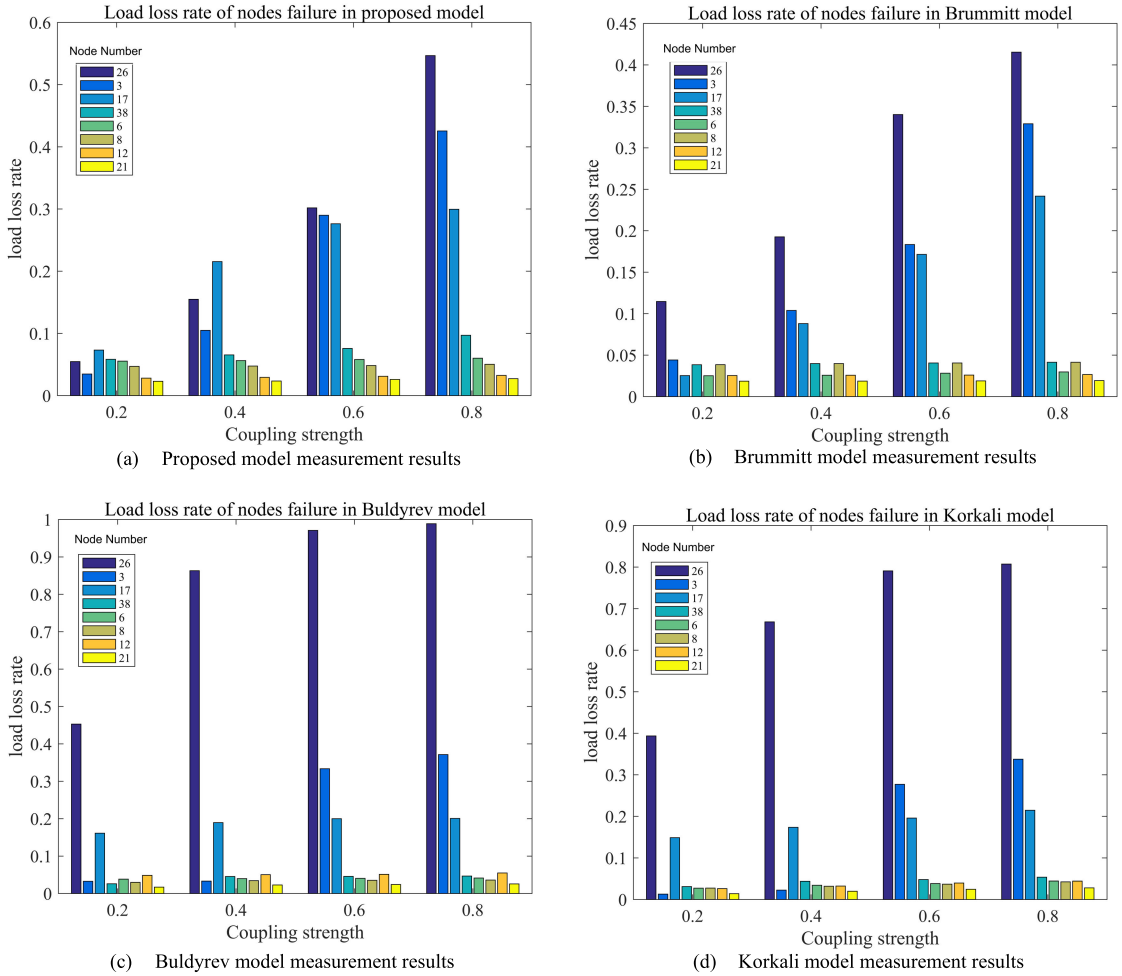

(a) Proposed model measurement results
(b) Brummitt model measurement results
(c) Buldyrev model measurement results
(d) Korkali model measurement results

FIGURE 7. **Influence measurement results of the four models.**

Under the model in this study, with an increase in the coupling strength ρ, the influence of the communication layer node increases, and the order of the influence of the node also changes. This is because when ρ is small, the communication layer failure mainly spreads in this layer. As ρ increases, the probability of physical layer coupling node failure increases, which affects the stability of the power flow in the physical layer and expands the influence. The results show that the effect of coupling strength on the model is consistent with the actual situation.

To further illustrate the accuracy and differentiation of the cascading failure model proposed in the application of the CPPS communication layer node impact measurement, this section compares the results with three typical cascading failure models.

1) RESULT ACCURACY

Because the goal of node influence measurement is to acquire the first K nodes, the communication layer nodes were ranked in descending order according to the measurement values generated by the cascading failure models. Kendall's Tau(τ)coefficient was used to measure the accuracy of the ranking results obtained by the model in this study. Equation 4-2 shows the τ calculation formula. The greater τ is, and the closer the score is to the other three models, the higher the accuracy of the model.

$$\boldsymbol{\tau} = \frac{\boldsymbol{Num_s} - \boldsymbol{Num_d}}{\frac{1}{2}\boldsymbol{n(n-1)}} \tag{4-2}$$

Num_s is the consistent logarithm, Num_d is the inconsistent logarithm, and the value of τ is between -1 and 1. A value of 1 indicates that the measurement results of node influence under the two indicators are completely consistent, and a value of -1 indicates that the results are completely inconsistent.

Figures 6(a-d) depict the consistency between the three classic cascading failure models and the model in this study under different experiment networks. Overall, the consistency between the model in this study and the three models was high, generally more than 0.7, indicating that the ranking results obtained by the model in this study were accurate and could be verified in multiple models.

Because of the different system factors considered by each model, the consistency relationship between our model and

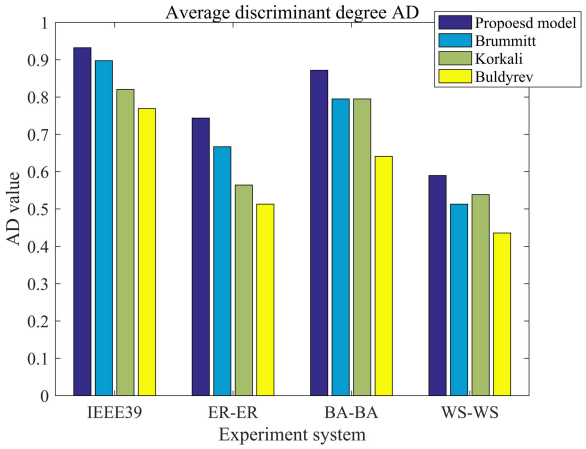

FIGURE 8. Average discrimination degree AD.

other models is analyzed in detail as follows: 1) The model consistency τ values between the Brummitt model and the proposed model are above 0.85, while the τ values in the Korkali model decrease along with decreases in ρ. Although the Brummitt and Korkali models are consistent with the model proposed in this paper, the physical failure propagation method and the communication transmission layer risk have not been considered. However, the Korkali model introduces a communication layer control function, making the model more useful; 2) Buldyrev model consistency is associated with its network structure. In the WS-WS dual-layer system, the sequencing result difference is greater, and the node importance difference is small. Only the Buldyrev model based on dependency node load power is used, and the physical sort results are sufficiently accurate. The above analysis shows that the differences in consistency relationships among the models are consistent with the differences in the model theories.

2) RESULT DISCRIMINATION

Node heterogeneity causes most nodes to have different influences. A good cascading failure model should reflect this heterogeneity and distinguish the influence of nodes as much as possible.

Fig.s 7 (a-d) illustrate the influence distribution of the first 8-bit nodes (except for the No. 16 dispatching center) obtained by the hierarchical model in the dual-layer IEEE 39 system. The influence of nodes in the system varies, and the influences of many nodes are concentrated between 0 and 0.1, which cannot explain the difference in the differentiation degree of each model. To quantitatively compare the discriminant effect of each model, the average discriminant degree, AD, is defined as follows:

$$AD = \sum_{i=1}^{n_\rho} \frac{dif_i}{n_\rho N_c} \tag{4-3}$$

n_ρ is the number of discrete points of the coupling strength ρ, dif_i is the number of different impact measurements given by the current ρ failure model, and N_c is the number of communication layer nodes. The greater the value of AD, the more detailed the classification of the influence of the cascading failure model on nodes. The maximum value of AD is 1, which indicates that all nodes in the network have different measurement values. The minimum value of AD is $1/N_C$, and the influence strength value of the communication layer nodes is the same. Figure 8 shows the AD values of four types of cascading failure models in the four experimental systems. It can be seen that the cascading failure model proposed in this paper has the best discrimination degree for measuring node influence.

V. CONCLUSION

The purpose of this paper is to propose an improved cascading failure modeling method for the Cyber Physical Power System. This method considers the operational characteristics of the communication layer of the CPPS; facilitates the analysis of the overall vulnerability of the system; provides guidance for system planning and design, optimization, and upgrading; and meets the development needs of the energy Internet.

However, for use with actual networks, the modeling granularity of the communication layer module needs to be refined. For example, in some access networks, the equipment has limited processing capacity, failure leads to the proliferation of network data, and communication congestion affects the failure development process. Therefore, the addition of smooth communication layer transmission can aid further research.

REFERENCES

[1] M. Ni, Y. S. Xue, H. Q. Tong, and M. L. Li, "A cyber physical power system co-simulation platform," in *Proc. Workshop Modeling Simulation Cyber-Phys. Energy Syst.*, Apr. 2018, pp. 1–5, doi: 10.1109/MSCPES.2018.8405398.

[2] R. V. Yohanandhan, R. M. Elavarasan, P. Manoharan, and L. Mihet-Popa, "Cyber-physical power system (CPPS): A review on modeling, simulation, and analysis with cyber security applications," *IEEE Access*, vol. 8, pp. 151019–151064, 2020, doi: 10.1109/Access.2020.3016826.

[3] G. C. Konstantopoulos, A. T. Alexandridis, and P. C. Papageorgiou, "Towards the integration of modern power systems into a cyber–physical framework," *Energies*, vol. 13, no. 9, p. 2169, May 2020, doi: 10.3390/en13092169.

[4] Y. Wu, L. Fu, F. Ma, and X. Hao, "Cyber-physical co-simulation of shipboard integrated power system based on optimized event-driven synchronization," *Electronics*, vol. 9, no. 3, p. 540, Mar. 2020, doi: 10.3390/electronics9030540.

[5] P. A. Oyewole and D. Jayaweera, "Power system security with cyber-physical power system operation," *IEEE Access*, vol. 8, pp. 179970–179982, 2020, doi: 10.1109/Access.2020.3028222.

[6] Y. Hu, Z. Jiang, Y. Sun, Y. Ding, C. Xu, and X. Jin, "Data transmission of cyber physical power system," *IOP Conf., Earth Environ. Sci.*, vol. 467, Apr. 2020, Art. no. 012113, doi: 10.1088/1755-1315/467/1/012113.

[7] S. Srinivasan, Ø. H. Holhjem, G. Marafioti, G. Mathisen, A. Maffei, G. Palmieri, L. Iannelli, and L. Glielmo, "Cyber-physical energy systems approach for engineering power system state estimation in smart grids," in *Soft Computing Applications* (Advances in Intelligent Systems and Computing), vol. 633. Cham, Switzerland: Springer, 2018, pp. 118–132, doi: 10.1007/978-3-319-62521-8_11.

[8] K. Chen, F. Wen, C. L. Tseng, M. Chen, Z. Yang, H. Zhao, and H. Shang, "A game theory-based approach for vulnerability analysis of a cyber-physical power system," *Energies*, vol. 12, no. 15, p. 3002, Aug. 2019, doi: 10.3390/en12153002.

[9] H. Guo, S. S. Yu, H. H. C. Iu, T. Fernando, and C. Zheng, "A complex network theory analytical approach to power system cascading failure—From a cyber-physical perspective," *Chaos, Interdiscipl. J. Nonlinear Sci.*, vol. 29, no. 5, May 2019, Art. no. 053111, doi: 10.1063/1.5092629.

[10] T. Zhao, D. Wang, D. Lu, Y. Zeng, and Y. Liu, "A risk assessment method for cascading failure caused by electric cyber-physical system (ECPS)," in *Proc. 5th Int. Conf. Electr. Utility Deregulation Restructuring Power Technol. (DRPT)*, Nov. 2015, pp. 787–791.

[11] M. Eskandari, L. Li, M. H. Moradi, P. Siano, and F. Blaabjerg, "Optimal voltage regulator for inverter interfaced distributed generation units part: Control system," *IEEE Trans. Sustain. Energy*, vol. 11, no. 4, pp. 2813–2824, Oct. 2020, doi: 10.1109/Tste.2020.2977330.

[12] S. Soltan, M. Yannakakis, and G. Zussman, "REACT to cyber attacks on power grids," *IEEE Trans. Netw. Sci. Eng.*, vol. 6, no. 3, pp. 459–473, Jul. 2019, doi: 10.1109/Tnse.2018.2837894.

[13] S. Hacks, A. Hacks, S. Katsikeas, B. Klaer, and R. Lagerstrom, "Creating meta attack language instances using ArchiMate: Applied to electric power and energy system cases," in *Proc. IEEE 23rd Int. Enterprise Distrib. Object Comput. Conf.*, Oct. 2019, pp. 88–97.

[14] Q. Xiao, Y. Jin, C. Dong, H. Jia, K. Hou, Q. Chen, A. F. Cupertino, R. Teodorescu, and T. Dragičević, "An improved power regulation method for a three-terminal hybrid AC/DC microgrid during module failure," *Int. J. Electr. Power Energy Syst.*, vol. 123, Dec. 2020, Art. no. 106330, doi: 10.1016/j.ijepes.2020.106330.

[15] C. Pu, P. Wu, and Y. Xia, "Vulnerability assessment of power grids against link-based attacks," *IEEE Trans. Circuits Syst. II, Exp. Briefs*, vol. 67, no. 10, pp. 2209–2213, Oct. 2020, doi: 10.1109/Tcsii.2019.2958313.

[16] T. Kerdphol, Y. Matsukawa, M. Watanabe, and Y. Mitani, "Application of PMUs to monitor large-scale PV penetration infeed on frequency of 60 Hz Japan power system: A case study from Kyushu island," *Electr. Power Syst. Res.*, vol. 185, Aug. 2020, Art. no. 106393, doi: 10.1016/j.epsr.2020.106393.

[17] T. Nesti, F. Sloothaak, and B. Zwart, "Emergence of scale-free blackout sizes in power grids," *Phys. Rev. Lett.*, vol. 125, no. 5, Jul. 2020, Art. no. 058301, doi: 10.1103/PhysRevLett.125.058301.

[18] L. A. Clarfeld, P. D. H. Hines, E. M. Hernandez, and M. J. Eppstein, "Risk of cascading blackouts given correlated component outages," *IEEE Trans. Netw. Sci. Eng.*, vol. 7, no. 3, pp. 1133–1144, Jul. 2020, doi: 10.1109/Tnse.2019.2910837.

[19] B. A. Carreras, V. E. Lynch, I. Dobson, and D. E. Newman, "Critical points and transitions in an electric power transmission model for cascading failure blackouts," *Chaos, Interdiscipl. J. Nonlinear Sci.*, vol. 12, no. 4, pp. 985–994, Dec. 2002, doi: 10.1063/1.1505810.

[20] C. D. Brummitt, R. M. D'Souza, and E. A. Leicht, "Suppressing cascades of load in interdependent networks," *Proc. Nat. Acad. Sci. USA*, vol. 109, no. 12, pp. E680–E689, Mar. 2012, doi: 10.1073/pnas.1110586109.

[21] S. V. Buldyrev, R. Parshani, G. Paul, H. E. Stanley, and S. Havlin, "Catastrophic cascade of failures in interdependent networks," *Nature*, vol. 464, no. 7291, pp. 1025–1028, Apr. 2010, doi: 10.1038/nature08932.

[22] M. Korkali, J. G. Veneman, B. F. Tivnan, J. P. Bagrow, and P. D. H. Hines, "Reducing cascading failure risk by increasing infrastructure network interdependence," *Sci. Rep.*, vol. 7, no. 1, Mar. 2017, doi: 10.1038/srep44499.

[23] M. Parandehgheibi, E. Modiano, and D. Hay, "Mitigating cascading failures in interdependent power grids and communication networks," in *Proc. IEEE Int. Conf. Smart Grid Commun. (SmartGridComm)*, Nov. 2014, pp. 242–247.

[24] G. Golnari and Z.-L. Zhang, "The effect of different couplings on mitigating failure cascades in interdependent networks," in *Proc. IEEE Conf. Comput. Commun. Workshops (INFOCOM WKSHPS)*, Apr. 2015, pp. 677–682.

[25] D. Liu, X. Zhang, and C. K. Tse, "A stochastic model for cascading failures in smart grid under cyber attack," in *Proc. IEEE 3rd Int. Future Energy Electron. Conf. ECCE Asia (IFEEC-ECCE Asia)*, Jun. 2017, pp. 783–788.

[26] D. Liu, X. Zhang, C. Zhan, and C. K. Tse, "Modeling of cascading failures in cyber-coupled power systems," in *Proc. IEEE Int. Symp. Circuits Syst. (ISCAS)*, May 2017, pp. 2283–2286.

[27] M. Rahnamay-Naeini and M. M. Hayat, "On the role of power-grid and communication-system interdependencies on cascading failures," in *Proc. IEEE Global Conf. Signal Inf. Process.*, Dec. 2013, pp. 527–530.

[28] J. Chen, J. S. Thorp, and I. Dobson, "Cascading dynamics and mitigation assessment in power system disturbances via a hidden failure model," *Int. J. Electr. Power Energy Syst.*, vol. 27, no. 4, pp. 318–326, May 2005, doi: 10.1016/j.ijepes.2004.12.003.

[29] Y. C. Lai, A. Motter, T. Nishikawa, K. Park, and L. Zhao, "Complex networks: Dynamics and security," *Pramana*, vol. 64, no. 4, pp. 483–502, Apr. 2005, doi: Doi.10.1007/Bf02706197.

[30] Z. Wang, G. Chen, L. Liu, and D. J. Hill, "Cascading risk assessment in power-communication interdependent networks," *Phys. A, Stat. Mech. Appl.*, vol. 540, Feb. 2020, Art. no. 120496, doi: 10.1016/j.physa.2019.01.065.

[31] G. Ishigaki, R. Gour, and J. P. Jue, "Improving the survivability of clustered interdependent networks by restructuring dependencies," *IEEE Trans. Commun.*, vol. 67, no. 4, pp. 2837–2848, Apr. 2019, doi: 10.1109/Tcomm.2018.2889983.

[32] M. Shahid, M. Khan, J. Xu, K. Hashmi, S. Habib, M. Mumtaz, and H. Tang, "A hierarchical control methodology for renewable DC microgrids supporting a variable communication network health," *Electronics*, vol. 7, no. 12, p. 418, Dec. 2018, doi: 10.3390/electronics7120418.

[33] R. A. Shuvro, Z. Wangt, P. Das, M. R. Naeini, and M. M. Hayat, "Modeling cascading-failures in power grids including communication and human operator impacts," in *Proc. IEEE Green Energy Smart Syst. Conf. (IGESSC)*, Nov. 2017, pp. 1–6.

[34] J. Guo, Y. Han, C. Guo, F. Lou, and Y. Wang, "Modeling and vulnerability analysis of cyber-physical power systems considering network topology and power flow properties," *Energies*, vol. 10, no. 1, p. 87, Jan. 2017, doi: 10.3390/en10010087.

[35] J. Banerjee, A. Das, and A. Sen, "A survey of interdependency models for critical infrastructure networks," *Nato Sci. Peace Secur.*, vol. 37, pp. 1–16, Feb. 2014, doi: 10.3233/978-1-61499-391-9-1.

[36] R. Cao, X. Dong, B. Wang, and K. Liu, "Discussion of protection and cascading outages from the viewpoint of communication," in *Proc. Int. Conf. Adv. Power Syst. Autom. Protection*, Oct. 2011, pp. 2430–2437. [Online]. Available: https://www.scopus.com/inward/record.uri?eid=2-s2.0-84860728357&doi=10.1109%2fAPAP.2011.6180833&partnerID=40&md5=0a2b0364595244b492845f4a3284a24a, doi: 10.1109/APAP.2011.6180833.

[37] J. Hu, J. Yu, J. Cao, M. Ni, and W. Yu, "Topological interactive analysis of power system and its communication module: A complex network approach," *Phys. A, Stat. Mech. Appl.*, vol. 416, pp. 99–111, Dec. 2014, doi: 10.1016/j.physa.2014.08.015.

[38] D. Zhou, J. Gao, H. E. Stanley, and S. Havlin, "Percolation of partially interdependent scale-free networks," *Phys. Rev. E, Stat. Phys. Plasmas Fluids Relat. Interdiscip. Top.*, vol. 87, no. 5, May 2013, Art. no. 052812, doi: 10.1103/PhysRevE.87.052812.

[39] Z. Huang, C. Wang, M. Stojmenovic, and A. Nayak, "Balancing system survivability and cost of smart grid via modeling cascading failures," *IEEE Trans. Emerg. Topics Comput.*, vol. 1, no. 1, pp. 45–56, Jun. 2013, doi: 10.1109/Tetc.2013.2273079.

[40] X. Gao, M. Peng, C. K. Tse, and H. Zhang, "A stochastic model of cascading failure dynamics in cyber-physical power systems," *IEEE Syst. J.*, vol. 14, no. 3, pp. 4626–4637, Sep. 2020, doi: 10.1109/Jsyst.2020.2964624.

[41] X. Zhang, D. Liu, C. Zhan, and C. K. Tse, "Effects of cyber coupling on cascading failures in power systems," *IEEE J. Emerg. Sel. Topics Circuits Syst.*, vol. 7, no. 2, pp. 228–238, Jun. 2017, doi: 10.1109/Jetcas.2017.2698163.

[42] O. V. G. Swathika and S. Hemamalini, "Prims aided Floyd Warshall algorithm for shortest path identification in microgrid," in *Emerging Trends in Electrical, Communications and Information Technologies* (Lecture Notes in Electrical Engineering), vol. 394. Singapore: Springer, 2017, pp. 283–291, doi: 10.1007/978-981-10-1540-3_30.

[43] R. D. Zimmerman, C. E. Murillo-Sanchez, and R. J. Thomas, "MATPOWER: Steady-state operations, planning, and analysis tools for power systems research and education," *IEEE Trans. Power Syst.*, vol. 26, no. 1, pp. 12–19, Feb. 2011, doi: 10.1109/Tpwrs.2010.2051168.

GENG ZHANG is currently pursuing the Ph.D. degree in communications and information system with Wuhan University, Wuhan, China. He is currently a Senior Engineer excellent experts of State Grid Corporation of China with the China Electric Power Research Institute Company Ltd., a member of TC06 (power information and communication) Standard Committee, State Grid Corporation of China, and a Deputy Secretary General with the Cable Network Technical Committee, IEEE PES Technical Committee. He has authored over 50 papers in different journals and conferences. He has successively established the Power Cyber Physics System Laboratory, State Grid Corporation of China. His research interests include power cyber physics systems, electric power communication networks, and energy internet information communication.

JIAWEN SHI received the M.S. degree in communication engineering from the Electronic Information School, Wuhan University, China.

Her research interests include simulation of cyber physical power systems and electric power communication networks.

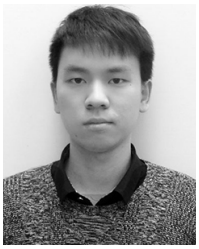

SHIYAN HUANG is currently pursuing the M.S. degree in communication engineering with the Electronic Information School, Wuhan University, China.

His research interests include simulation of cyber physical power systems and optical transmission networks.

JIYE WANG is currently a General Manager with the China Electric Power Research Institute Company Ltd. He is also the Dean of the State Grid Energy Internet Technology Research Institute, the Ph.D. Supervisor with the China Electric Power Research Institute, and a part-time Ph.D. Supervisor with Wuhan University and the Beijing University of Posts and Telecommunications. He is the Chairman of the Energy Internet Special Committee of China Communication Society and the China Artificial Intelligence Chairman of the Smart Energy Professional Committee of Energy Society. He has authored over 40 papers in different journals and conferences. His research interests include power cyber physics systems, electric power communication networks, and energy internet.

HAO JIANG received the B.Eng. degree in communication engineering and the M.Eng. and Ph.D. degrees in communication and information systems from Wuhan University, China, in 1999, 2001, and 2004, respectively.

He undertook his Postdoctoral Research Work with LIMOS, Clermont-Ferrand, France, from 2004 to 2005. He was a Visiting Professor with the University of Calgary, Canada, and ISIMA, B. Pascal University, France. He is currently a Professor with Wuhan University. He has authored over 60 papers in different journals and conferences. His research interests include mobile ad hoc networks and mobile big data.